Journal of Statistical Physics, Vol. 49, Nos. 1/2, 1987

Nonequilibrium Second-Order Phase Transitions in Stochastic Lattice Systems: A Finite-Size Scaling Analysis in Two Dimensions

J. L. Vallés[1,2] and J. Marro[1,3]

Received December 17, 1986; revision received May 7, 1987

Two-dimensional lattice-gas models with attractive interactions and particle-conserving happing dynamics under the influence of a very large external electric field along a principal axis are studied in the case of a critical density. A finite-size scaling analysis allows the evaluation of critical indexes for the infinite system as $\beta = 0.230 \pm 0.003$, $\nu = 0.55 \pm 0.2$, and $\alpha \approx 0$. We also describe some qualitative features of the system evolution and the existence of certain anisotropic order even well above the critical temperature in the case of finite lattices.

KEY WORDS: Stochastic lattice-gas model; stationary nonequilibrium states; fast ionic conductors; nonequilibrium critical behavior.

1. INTRODUCTION

The lattice-gas version of the Ising model with particle-conserving hopping dynamics under the influence of an external electric field can be used to model the so-called fast ionic or superionic conductors[4]; in addition, this model is convenient for the analysis of many interesting general properties of stationary nonequilibrium states, such as the occurrence of instabilities and "phase transitions," for which there is no statistical mechanics formalism comparable to the equilibrium Gibbs ensemble theory.

The latter difficulty is partially reflected, for instance, in the fact that,

[1] Departamento de Física Fonamental, Universitat de Barcelona, E-08028 Barcelona, Spain.
[2] Present address: Courant Institute of Mathematical Sciences, New York University, 251 Mercer Street, New York, New York 10012.
[3] Present address: Departamento de Física, Facultad de Ciencias, Universidad de Granada, Granada, Spain.
[4] See Ref. 1 (henceforth referred to as III) for a bibliography and a description of some general properties of fast ionic conductors.

0022-4715/87/1000-0089$05.00/0

excluding the exact solution under certain limiting conditions,[2,3] the rigorous results for that model are confined to rather general properties,[4] while most details have only emerged recently via computer simulations.[4–7] These have shown in particular that, in the case of a two-dimensional periodic lattice with attractive interactions between the particles (the case where the computer data are most reliable at present), a very strong uniform electric field $\mathbf{E}$ along one of the principal axes produces striplike configurations in the direction of $\mathbf{E}$ below some temperature T_c^*, this being larger than the Onsager critical temperature $T_c \approx 2.2692\ J/k_B$, which characterizes the corresponding equilibrium situation (i.e., $E=0$). They also revealed that the anisotropic phase segregation has a critical point (at T_c^* with a half-filled lattice) and, apparently, a new (nonequilibrium) universality class in two dimensions differing from both the Onsager–Ising class and the Landau classical one (Ref. 6; henceforth referred to as I). As a matter of fact, previous results for a fluid under shear model[8] and parallel studies concerning reaction–diffusion Ising models[9,10] and continuous versions of the model of interest here[11–13] seem to confirm that the nonequilibrium critical behavior may be more varied than the equilibrium one.

Those studies also made it evident that the interesting field of nonequilibrium critical behavior needs further consideration. In particular, the nonclassical critical behavior reported in I for the two-dimensional fast ionic conductor model needs to be confirmed, given that (nonequilibrium) classical behavior is found more generally.[2,3,8,12,13] This motivated the present study in two-dimensions (and a similar study just started in three dimensions, where previous, very limited Monte Carlo data[7] suggested nonclassical behavior also).

We report in this paper on an extensive finite-size scaling analysis of the two-dimensional fast ionic conductor model near the corresponding critical point. Essentially, we confirm the qualitative results in I. We also describe various correlation functions, and evaluate the critical exponents β, ν, and, to some extent, α. In a companion paper (III) we study the first-order phase transitions occurring for off-critical densities, evaluate coexistence and spinodal lines, and make some comparisons with related experimental observations.

2. SOME DETAILS OF THE MODEL, COMPUTATIONS, AND EVOLUTION

The model of interest here is the basic one considered previously in I. It consists of a square lattice $L \times L$ with periodic boundary conditions whose sites can be either occupied by a particle to be intepreted as a positive ion, a situation represented by setting the occupation variable at

that site $n_i = 1$, or empty, $n_i = 0$, $i = 1, 2, \ldots, N = L^2$. A given initial configuration $n_0 = \{n_i\}$ with density $\rho = N^{-1} \sum n_i = 1/2$ evolves according to a stochastic hopping dynamics with conserved ρ, i.e., ions hop to nearest neighbor (n.n.) empty sites according to the transition probabilities per unit time

$$p = \min\{1, \exp[-(\delta H + E)/k_B T]\} \tag{2.1}$$

Here δH represents the change in the configurational system energy,

$$H(\{n_i\}) = -4J \sum_{\text{n.n. pairs}} n_i n_j, \qquad J > 0 \tag{2.2}$$

produced by the jump, and E stands for a very large uniform external electric field along one of the principal directions of the lattice; namely, we set $E/k_B T = \pm 15$ for jumps in the directions $\pm \hat{x}$, respectively, corresponding in practice to having an "infinite" electric field in the $+\hat{x}$ direction such that no jumps occur in the $-\hat{x}$ direction, and $E = 0$ for jumps in the perpendicular directions $\pm \hat{y}$. The transition probabilities (2.1), which satisfy detailed balance locally,[4] can be viewed as a generalization of the usual Metropolis dynamics when $E \neq 0$. One may also think of other dynamics as well, but it seems that the most interesting features of the corresponding nonequilibrium phase transition in this case are already contained in the present version of the model.[6,7] As a matter of fact, they are mainly associated with the existence of the (inkfinite) external electric field **E** suppressing the jumps in the $-\hat{x}$ direction, thus producing, as a consequence of the periodic boundary conditions, a simple (nonequilibrium) steady state characterized by an ion current in the field direction. Notice that the system also interacts, stochastically, with a heat reservoir at temperature T, which serves in particular to maintain the steady state absorbing the heat generated by the current.

The highly anisotropic phase segregation induced by the field **E** below some critical temperature T_c^* (see Fig. 1 for typical configurations during the stationary nonequilibrium states) can be investigated by considering the order parameter

$$\begin{aligned} m &= [\langle M_x^2 \rangle_T - \langle M_y^2 \rangle_T]^{1/2} \\ M_{x(y)}^2 &= L^{-1} \sum_{y(x)} \left[L^{-1} \sum_{x(y)} (2n_{xy} - 1) \right]^2 \end{aligned} \tag{2.3}$$

where $\langle \cdot \rangle_T$ denotes the "canonical" ensemble average at temperature T produced by (2.1); this measures the density difference between fluid (striplike) and vapor (isotropic) phases.

The present computations refer to lattices $L = 10$, 15, 30, 50, and 100; they also involve some "confidence" runs for $L = 300$ and much larger

statistics when $L = 50$ than in I. The initial configurations n_0 for $L \leqslant 30$ are always random, as if the system was quenched to the temperature T in the selected transition probability, Eq. (2.1), from an "infinite" temperature (i.e., random) initial state. Below some apparent criticl temperature $T_c^*(L)$, the system then evolves monotonically (smooth variations of m) toward one-strip stationary states, which are reached in practice in a relatively short time measured in Monte Carlo (MC) steps, i.e., number of attempted jumps divided by N. The data for $L = 50$, on the other hand, were obtained by extending the runs reported previously in I. Most of the runs in this case showed two-strip intermediate states, suddenly decaying into one-strip states after rather large evolutions (cf. Fig. 1 in I); Fig. 2a presents a typical evolution of the order parameter in those cases, revealing that the mean values characterizing each situation are within the fluctuations of the other.

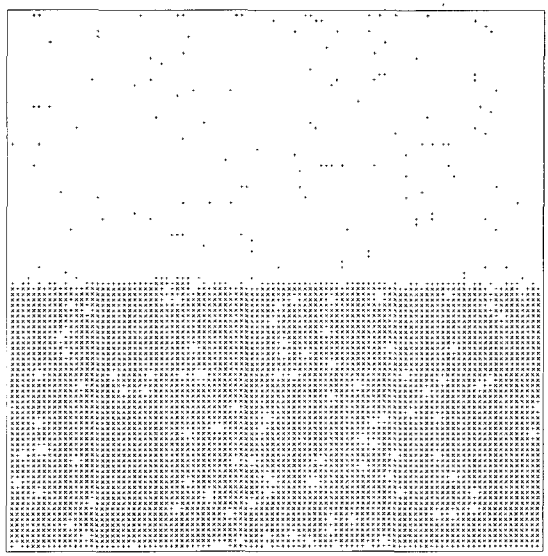

(a)

Fig. 1. Some typical configurations of the system with $\rho = 0.5$ under an infinite uniform external electric field along the horizontal direction. In order to emphasize the interphase shape and the clustering, the particles (ions) surrounded by other particles at all the n.n. positions are represented by crosses, while the pluses represent particles having at least a n.n. hole. (a) A typical configuration during the final steady state for $L = 100$ and $T = 0.8T_c$. (b) Same for $T = 1.2T_c$. (c) Same for $T = 1.3T_c$, still below the critical temperature T_c^* in the presence of the field. (d) Same for $T = 1.45T_c$, above T_c^*. (e) Intermediate multistrip states for $L = 100$ and $T = 1.1T_c$ after 6000 MC steps in the case of a quench from infinite temperature; this never decayed into a one-strip state during our evolutions. (f) Same as in (e), but for $L = 300$.

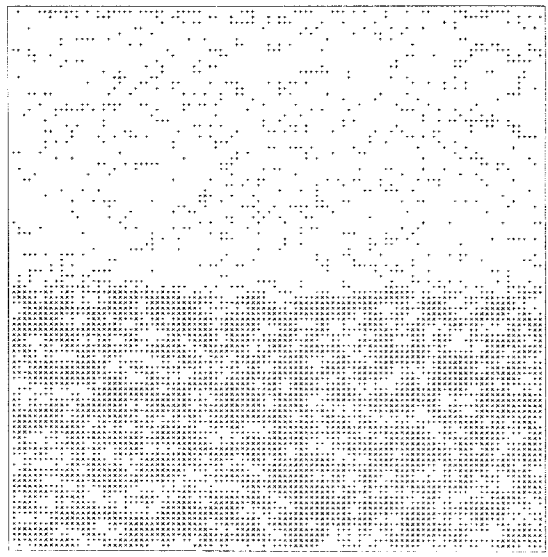

(b)

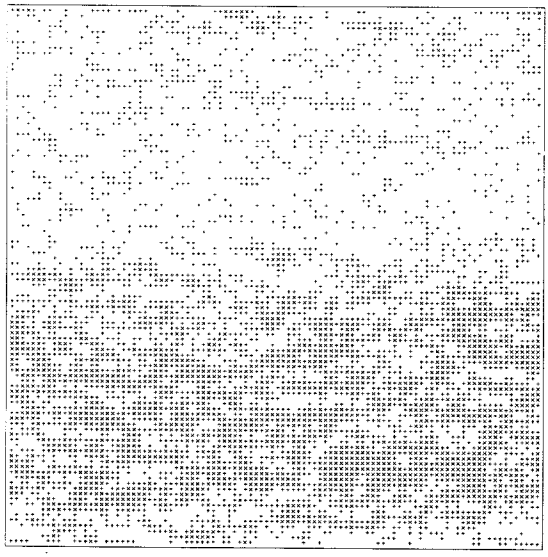

(c)

Fig. 1 (*continued*)

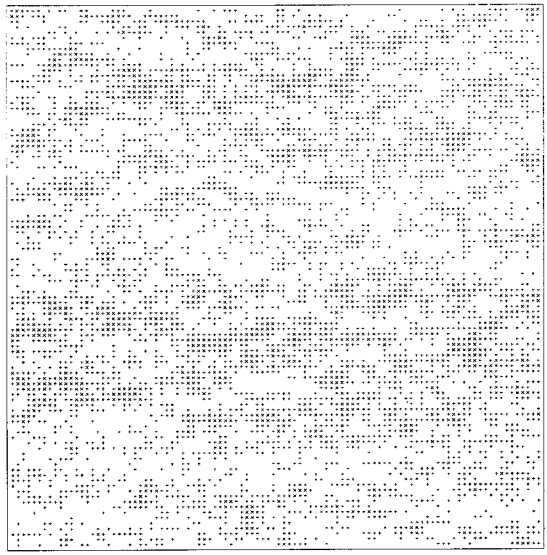

(d)

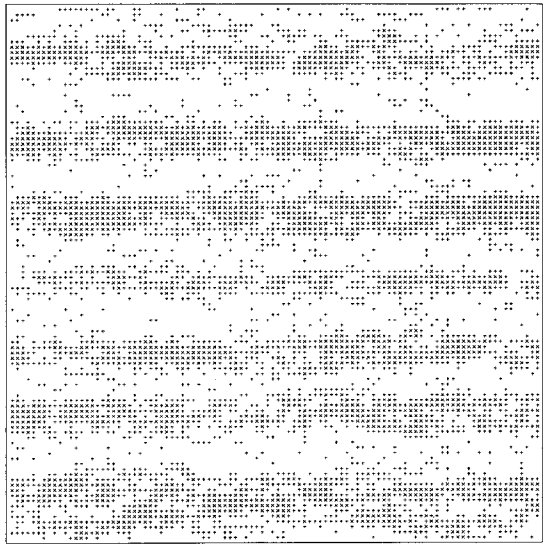

(e)

Fig. 1 (*continued*)

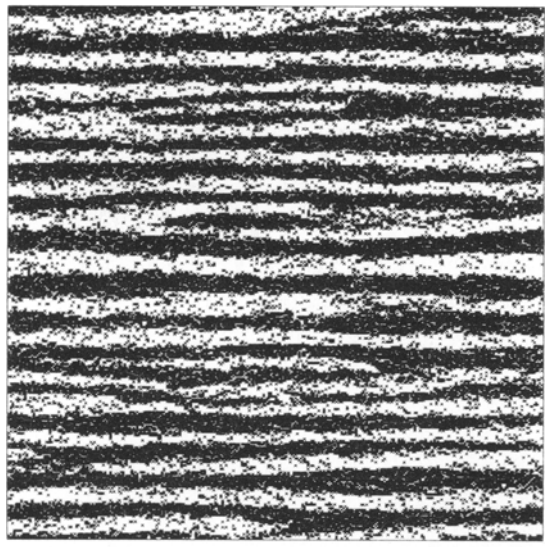

(f)

Fig. 1 (*continued*)

The system was never seen to escape from those "metastable" states (which essentially differ from the metastable states to be reported in III when $\rho < 1/2$) during a few of our runs at low temperatures, and we had to manipulate some system configurations for $L = 50$ to create artificial one-strip states in those cases.

It seems that the nature of the intermediate multistrip states strongly depends on system size. On the one hand, the number of strips clearly increases with L, as shown by Figs. 1e and 1f, collecting two typical configurations which were never seen to decay. On the other hand, the corresponding time of excape probably diverges as $L \to \infty$; in fact, we were unable to observe the decay toward one-strip states during very large evolutions in the case of systems with $L \geqslant 100$ quenched from infinite temperature. Thus, in order to obtain the reported information concerning stationary one-strip states, we usually started the evolutions for $L \geqslant 100$ by heating up a (zero-temperature) configuration in which all the particles were in a single, compact symmetric strip. We never observed during these processes a one-strip state to split into several strips; a typical evolution is depicted in Fig. 2b.

As a general fact, it is also noticeable that the present Monte Carlo computation required one order-of-magnitude more statistics, in order to obtain good Gaussians for most of the variables of interest, then ordinary

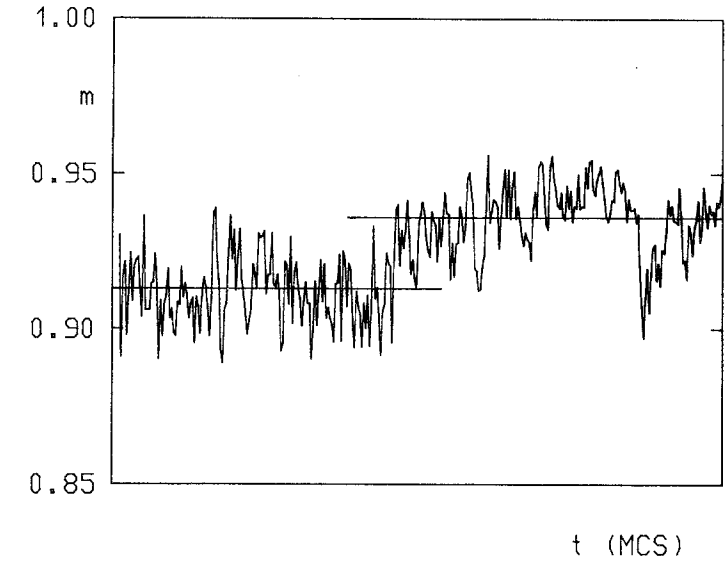

(a)

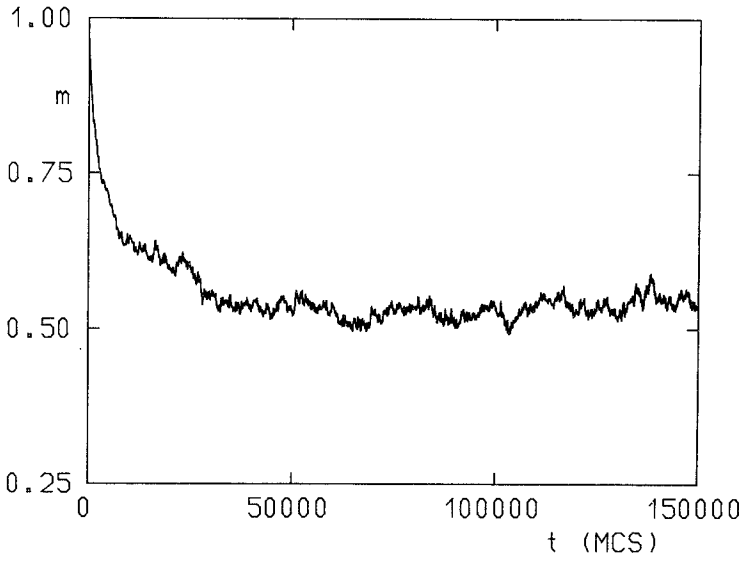

(b)

Fig. 2. (a) Time evolution of the order parameter in a typical run for $L = 50$ and $T = 0.8T_c$. The initial part of the evolution (around 35,000 MC steps) corresponds to a two-strip state, which finally decays into the real, stationary one-strip state. The straight lines represent the corresponding mean values, $m = 0.913$ and 0.936, respectively. (b) Same for $L = 100$ and $T = 1.3T_c$, near $T_c^*(L)$, in the case of a system heated from zero temperature.

MC computations for the Ising model ($E=0$). Actually, the duration of our runs extended from 10^5 to 3×10^6 MC steps, each mean value being an average of more than 2000 (practically uncorrelated) measurements.

3. DESCRIPTION OF DATA

The anisotropy observed during the phase segregation of the system compels one in principle to consider separately the values of most relevant quantities along the two principal directions of the lattice, the direction $\hat{x}$ of the field and the perpendicular direction $\hat{y}$.

The configurational system energy per lattice site as defined in Eq. (2.2),

$$u(T)=\langle H\rangle_T/(-JN)=u_x+u_y \tag{3.1}$$

can be related to the number of particle–hole bonds (to be represented by $e=e_x+e_y$) via the equations

$$u=2-2e, \qquad u_{x(y)}=1-2e_{x(y)} \tag{3.2}$$

As the temperature is increased, $T\to\infty$ (random configuration), one should expect $e_x\approx e_y$, and u_x, u_y, and $u\to0$. This is indeed suggested by Fig. 3, collecting our data for $x_x(T)$ and $u_y(T)$ as a function of L. The data also reveal that finite-size effects are very small for $T>T_c^*$, the latter interpreted as the temperature for which there is a (sudden) change in the corresponding second derivative for large enough lattices, while they are very important for $T<T_c^*$. The latter dependence is approximately linear with L^{-1} when $L\geqslant15$, both for u_x and u_y, a behavior which essentially differs from the one in the equilibrium case with periodic boundary conditions. On the contrary, that and other finite-size effects in our model closely resemble, at least approximately, the situation found in the equilibrium case with free edges,[14] probably as one should expect after some simple thought. Thus, the data in Fig. 3 easily allow us to obtain the extrapolated values of the energy for $L\to\infty$ (Fig. 4) when making plots of $u_{x(y)}$ versus L^{-1}.

Most important to our purposes here is the average current in the direction of the field $j_x(T)$, defined as the number of actual jumps per site performed in the direction $\hat{x}$ per unit time. This, however, is simply related to $u_x(T)$. Let us consider for a moment the generalized version of the model studied in I, where the jumps in the direction of the field are attempted with a frequency Γ times larger than the perpendicular jumps; in a d-dimensional space, the fraction of attempted moves in the direction $+\hat{x}$ is $f_x(\Gamma)=\Gamma/2(\Gamma+d-1)$, and it follows for the infinite field that

$$j_x(T)=e_x(T)\,f_x(\Gamma) \tag{3.3}$$

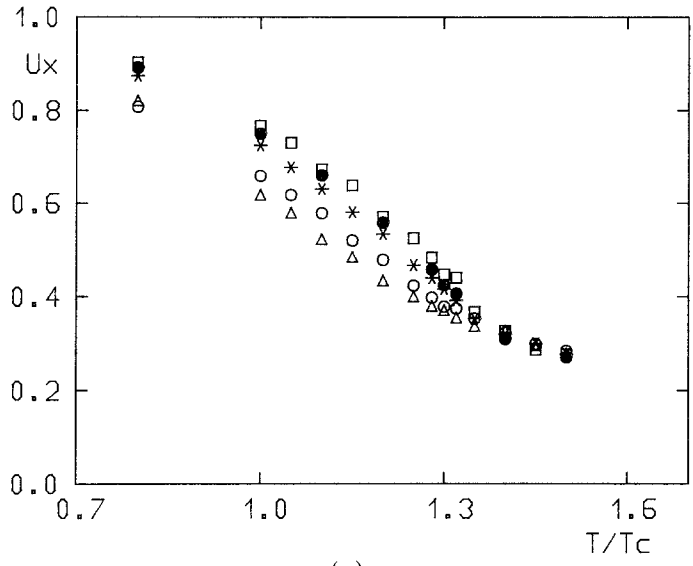

(a)

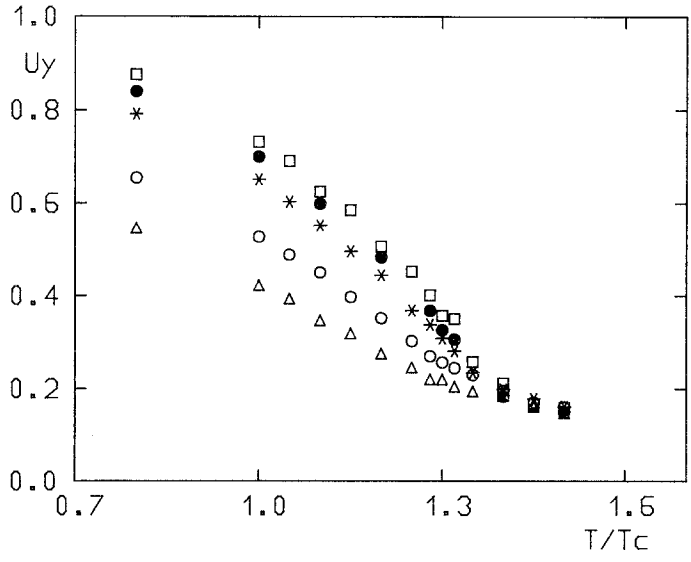

(b)

Fig. 3. (a) The configurational energy u_x parallel to the field as a function of temperature for different lattice sites: $L = (\triangle)$ 10, $(\bigcirc)$ 15, $(*)$ 30, $(\bullet)$ 50, and $(\square)$ 100. (b) Same for u_y.

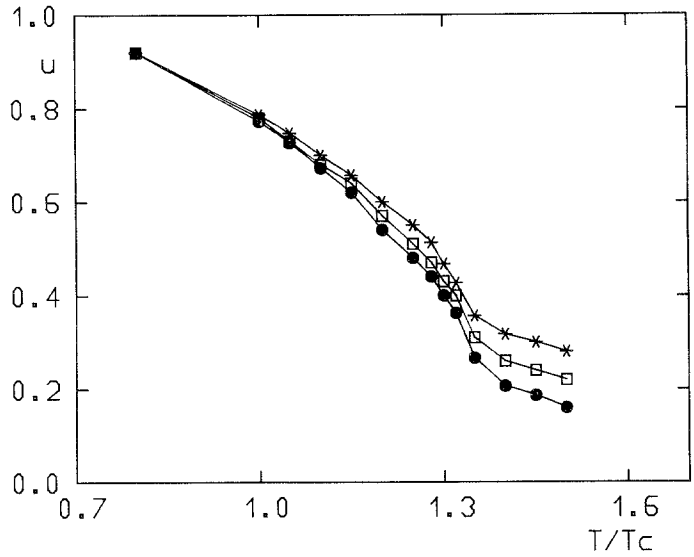

Fig. 4. The configurational energies (□) $u/2$, (∗) u_x, and y (●) u_y for the infinite lattice as extrapolated from the data in Fig. 3; cf. Eq. (3.1).

or $j_x(T) = e_x(T)/4$ and $j_x(\infty) = 1/8$ in the present case ($\Gamma = 1$). Figure 4 in I reports some independent data for $j_x(T)$ in the case of finite lattices; we shall specifically refer to the behavior of $j_x(T)$ for the infinite system when making comparisons with experimental results in Section 5 of paper III.

The behavior of the order parameter for the nonequilibrium phase transition, $m(T)$ as defined in Eq. (2.3), is shown in Fig. 5 as a function of L. One observes here strong finite-size effects both above and below T_c^* and, in particular, that the situation resembles again the equilibrium case with free edges. More precisely, one has approximately, excluding the smaller values of L, that m behaves linearly with L^{-1} for $T < T_c^*$ and with L^n, $n \approx -0.2$, for $T > T_c^*$; this is confirmed later, where n is given a physical meaning.

The simple phenomenological dependence on L shown by $m(T)$ also allows, as in the case of $u(T)$, the computation of the order parameter for the infinite system, say $m^*(T)$. The extrapolated values for $m^*(T)$ can then be used to obtain estimations for the corresponding critical exponent β and temperature T_c^* (to be confirmed later by the finite-size scaling analysis). The most reliable way of doing so here is probably by making plots of $(m^*)^{1/\beta}$ versus T for different trial values of β, looking for straihgt lines. [This procedure is indeed more sensitive than the usual $\log m^*$ versus $\log(1 - T/T_c^*)$ plot, and it involves no *a priori* assumption about T_c^*

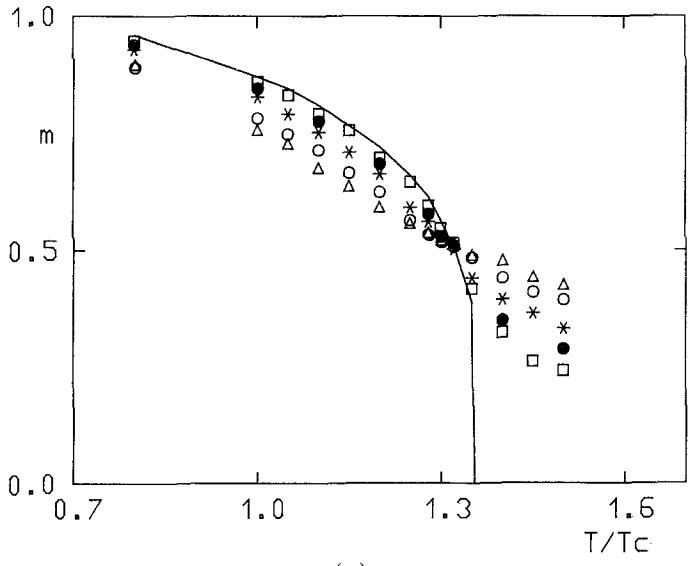

(a)

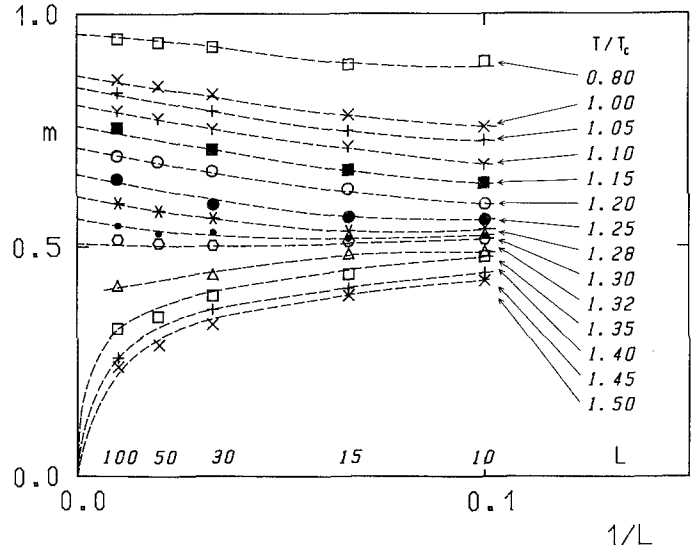

(b)

Fig. 5. The order parameter as defined in Eq. (2.3) as (a) a function of T/T_c for different sizes (same symbols as in Fig. 3), and (b) as a function of L^{-1} for different temperatures.

(except, of course, or drawing of the dashed lines in Fig. 5b, which is well-founded based on the previous experience about L dependences[14] and on the behavior of our "confidence" runs for $L=300$; see below); it should also be noticed that making $m^{*1/\beta}$ versus T plots in some related familiar situations, such as with the Onsager solution for the two-dimensional Ising model and the corresponding mean-field solution, only yields straight lines over rather wide temperature ranges, namely from $0.7T_c$ to T_c in the Onsager case and from $0.8T_c$ to T_c in the mean-field case, when using the respective correct values for β.] Such plots definitely show that neither $\beta=1/8$ nor $\beta=1/2$ can produce the expected linear behaviors for $m^{*1/\beta}$; instead, the best straight line extending over the expected temperature range is found (Fig. 6) for

$$\beta = 0.230 \pm 0.003 \tag{3.4a}$$

That line then intersects the horizontal axis at

$$T_c^* = (1.355 \pm 0.003)T_c \tag{3.4b}$$

which is quite consistent with the situation depicted by Fig. 4 and with the rest of the data for the infinite lattice. Those values, which are also

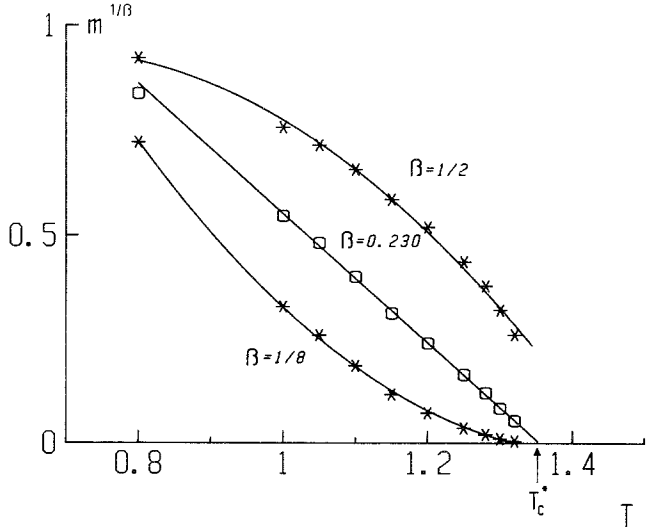

Fig. 6. The data for the order parameter m^* corresponding to the infinite lattice, as obtained by extrapolating to $L \to \infty$ the data in Fig. 5, plotted for different hypotheses for β. The case $\beta=0.23$ produces the best straight line over the expected temperature range and extrapolates to a value of T_c^* consistent with the rest of the data.

consistent with the one reported in I for the case $L = 50$, namely $\beta = 0.23 \pm 0.02$ and $T_c^* = 1.33 \pm 0.02$, produce an impressive linear behavior over more than three decades in the familiar $\log m^*$ versus $\log(1 - T/T_c^*)$ plot.[10] The corresponding thermodynamic amplitude following from the previous analysis is $B = 1.186 \pm 0.03$. We may also mention that the value (3.4b) was further confirmed by performing some (relatively) short) evolutions of the system with $L = 300$: these never reached the stationary state (actually, they revealed critical slowing down around $1.35T_c$), but the time evolution of the order parameter was consistent with the dashed lines drawn in Fig. 5b.

One may define a specific heat C as the temperature derivative of the energy $u(T)$. The results for several finite lattices as well as for the infinite system are shown in Fig. 7; this is obtained from the data in Figs. 3 and 4 by first making a smooth cubic or spline interpolation such that the involved nodes are located, trying preferably to reproduce correctly the sign and variations of the second derivative at each temperature. Again, the behavior in Fig. 7 is similar to the one shown by the equilibrium model with free edges.[14] On the other hand, a similar study trying to obtain "directional specific heats" from $u_x(T)$ and $u_y(T)$ produces no new noticeable results. It seems more interesting to compare the above behavior with that of the response functions C' and X' obtained, respectively, from the mean squared fluctuations of the u and m data. The results are shown by Fig. 8, where, apart from some (small) noise, it is revealed that the

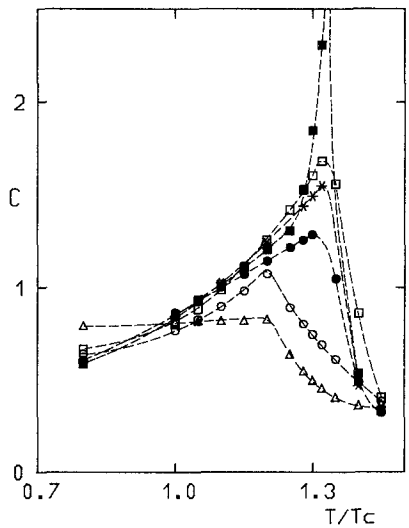

Fig. 7. The specific heat, defined as the temperature derivative of the energy u, for different sizes. Same symbols as in Fig. 3. (■) The infinite system, from the data in Fig. 4.

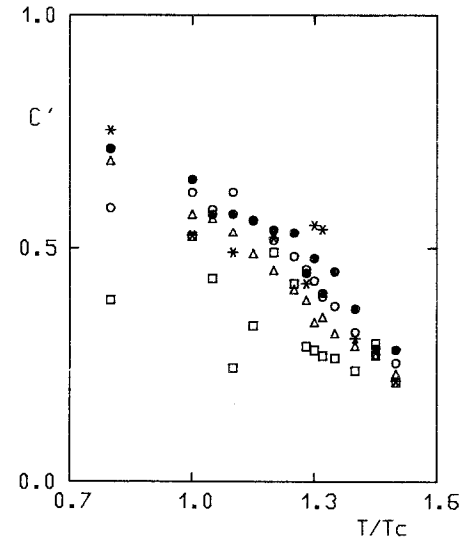

(a)

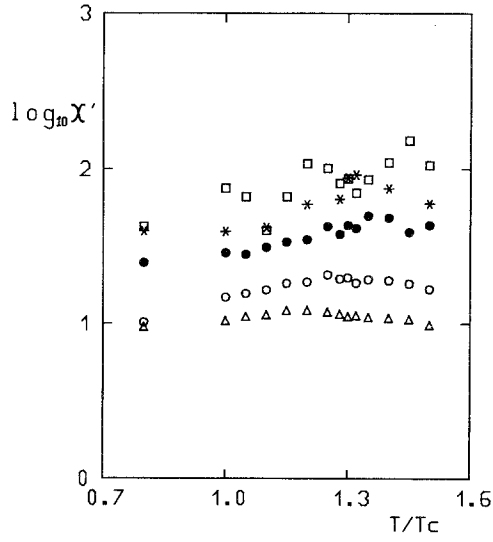

(b)

Fig. 8. (a) The specific heat and (b) the ordering susceptibility, obtained assuming a fluctuation theorem holds, for different sizes. Same symbols as in Fig. 3.

validity of fluctuation theorems seems to break down in the present non-equilibrium situation. Actually, the detailed balance condition only holds locally in the model, and the external electric field energy cannot be included in the Hamiltonian, so that there is no proof of the microscopic reversibility leading to the fluctuation-dissipation theorem.[3,4,12,15]

4. SCALING ANALYSIS

The strong finite-size effects reported above suggest that a detailed scaling analysis of the data with L and T be performed referring specifically to the present anisotropic case. We first introduce the hypothesis, first assumed and roughly confirmed by Katz[16] in a MC renormalization group computation, that there is a unique correlation length critical exponent ν in the problem. This assumption turns out to be consistent with our data in the sense that we never observed indications to the contrary (e.g., when comparing scaling behavior above and below the critical temperatur), and that introducing independent longitudinal and transverse correlation lengths produces no better results than the ones reported below (3.g., Fig. 12); see also Section 5 including an independent study of correlations.

Let us define a "critical temperature" for the finite system $T_c^*(L)$ as the one locating the peak of the specific heat in Fig. 7 or the most rapid change of the slope in Fig. 3. According to the above hypothesis,[14,17] this will be assumed to be characterized also by the condition that the relevant correlation length satisfies $\xi[T_c^*(L)] \approx L$ and consequently

$$1 - T_c^*(L)/T_c^* \approx aL^{-1/\nu} \tag{4.1}$$

where T_c^* represents the limit of $T_c^*(L)$ as $L \to \infty$. The fact that ξ is *the relevant* correlation length may be interpreted in several ways: ξ is an effective parameter describing the competition between longitudinal and transverse correlation effects, ξ is the longitudinal correlation length so that the longitudinal correlations dominate the critical behavior and render rather irrelevant the correlations along the direction perpendicular to the field, or the longitudinal and transverse correlation lengths are essentially proportional to each other near T_c^*. Figure 9 shows the consistency of the data with Eq. (4.1) when $T_c = 1.355 T_c$ and $\nu = 0.55$, which is the value reported in this paper. The fact that it follows that $a > 0$ ($a = 0.66$) in Eq. (4.1) from Fig. 9 is also a feature of the equilibrium two-dimensional Ising model with free edges, while the corresponding case with periodic boundary conditions is characterized by $a < 0$.[14]

Let $A_L(T)$ represent a physical quantity such that as $L \to \infty$ it has, say, an algebraic singularity $A_s(T) \approx A\varepsilon^{-\sigma}$ when $\varepsilon \to 0$; here ε is defined in

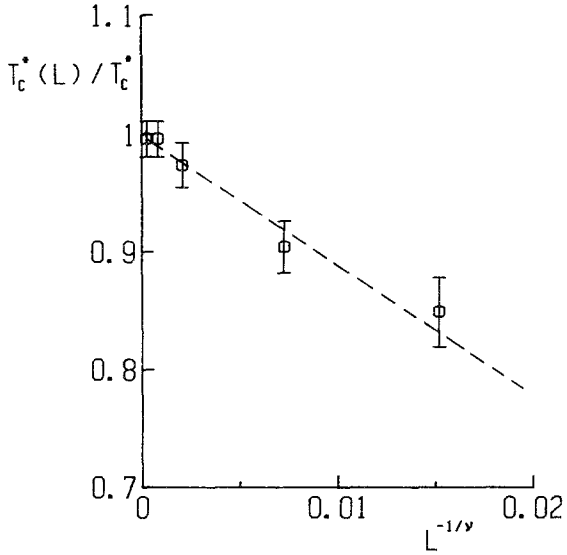

Fig. 9. The values for the "critical temperature" $T_c^*(L)$ characterizing the peaks in Fig. 7, shown to be consistent with Eq. (4.1) when T_c^* is given by Eq. (3.4b) and $\nu = 0.55$.

the usual way according to whether one considers $\varepsilon \to 0^+$ or 0^-. Homogeneity of the thermodynamic functions then leads to the usual scaling behavior[17]

$$A_L(T) = L^{\sigma/\nu} X(x), \qquad x = \varepsilon L^{1/\nu} \tag{4.2}$$

where it is required that $x \approx$ const for small x and $X(x) \approx Ax^{-\sigma}$ at large enough values of x, i.e., for $\varepsilon \ll 1$ and $L \to \infty$. One may expect (4.2) to be valid in the presence of anisotropic effects, except that the scaling functions should then include important "surface contribution,"[14] as described in the preceding sections. The anisotropy in the present case is not associated with any geometric parameter,[14] but with an intrinsic property of the model and one may simply expect

$$X(x) \approx Ax^{-\sigma} + A_s x^{-\sigma} \tag{4.3}$$

at large x.

The specific anisotropic contributions to the scaling functions may in principle be related to the observed general behavior of $A_L(T)$ with L for large L near the critical temperature. For instance, Eqs. (4.2) and (4.3) read in the case of the order parameter

$$m_L = L^{-\beta/\nu}(Bx^{\beta} + B_s x^{\beta_s}), \qquad T < T_c^* \tag{4.4}$$

and

$$m_L = B'_s(x')^{\beta'_s}, \qquad T > T_c^* \tag{4.5}$$

where the prime indicates that the corresponding quantity is defined above T_c^*. The observations, reported in Section 3, that $\Delta m \equiv m_L - m_\infty \approx L^{-1}$ below T_c^* and $\Delta m \approx L^n$ above T_c^* then lead, respectively, to $\beta_s = \beta - \nu$ and $\beta'_s = n\nu$. Thus, in order to compute these quantities in practice, one may proceed, for instance, as follows. Below T_c^* one has from Eq. (4.4) that

$$B - m_L \varepsilon^{-\beta} = -B_s x^{\beta_s - \beta} = -B_s L^{-1} \varepsilon^{-\nu} \tag{4.6}$$

so that a plot of $\ln(B - m_L \varepsilon^{-\beta}) - \ln(-B_s L^{-1})$ versus $\ln \varepsilon$ should produce a straight line of slope $-\nu$; the data confirm this, leading to the value

$$\nu = 0.55 \begin{cases} +0.20 \\ -0.05 \end{cases} \tag{4.7}$$

where we are overestimating the upper error bar following from the corresponding least squares fit in order to account also for our errors on B, β, and T_c^* as given in Section 3 and for the fact that increasing ν from 0.55 produces better scaling results later on than decreasing it. Now, according again to Eq. (4.6), a plot of $B - m_L \varepsilon^{-\beta}$ versus x will give $\beta_s - \beta$ and thus β_s; this, which happens to be noisier than the one before, is shown by Fig. 10; we obtain $\beta_s = -0.32$ and $B_s = -0.77$. The fact that

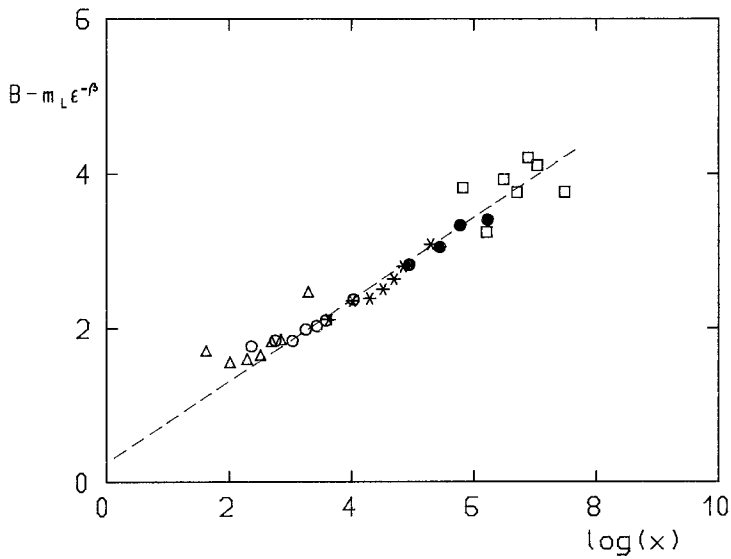

Fig. 10. Logarithmic representation of $B - m_L \varepsilon^{-\beta}$ versus $x = \varepsilon L^{1/\nu}$ below T_c^* to obtain $\beta_s - \beta$ and B_s in Eq. (4.6). Here $L = (\triangle)\ 10$, $(\bigcirc)\ 50$, and $(\square)\ 100$.

$B_s < 0$ is a characteristic of the present model, which is in contrast with the equilibrium case with periodic boundary conditions, and simply reflects that $\Delta m \approx a(\varepsilon)L^{-1}$, $a < 0$. Above T_c^* the situation is even simpler; it follows from Eq. (4.5) that a plot of m_L versus x' may give the exponent β_s'. This is shown by Fig. 11, producing $\beta_s' = -0.11$, which equals $n\nu$ with $n = -0.2$, and $B_s' = 0.52$.

The values obtained in this way be used now to test th suggested global scaling behavior, Eqs. (4.4) and (4.5). The result is quite convincing; this is shown by Fig. 12, where we only include the data for $x > 4$ below T_c^* and $x < 140$ above T_c^*. That is, scaling breaks down below T_c^* for very small values of x, where $\xi \gg L$ and finite-size effects are too strong, while we do not observe deviations from scaling in the range $4 < x \lesssim 1000$; above T_c^*, on the contrary, very large values of x tend to deviate from the behavior (4.5) given that finite-size effects are then very small and independent of temperature. Also, scaling tends to fail very near T_c^*, say for $x < 1.5$, probably because the expected changeover of m_L near T_c^* is not well reproduced by the computer simulation data.

The specific heat and ordering susceptibility obtained as the corresponding derivatives of the energy and order parameter may in principle be analyzed following the trend suggested by Eqs. (4.2) and (4.3) with some obvious changes. Nevertheless, the procedure to obtain those

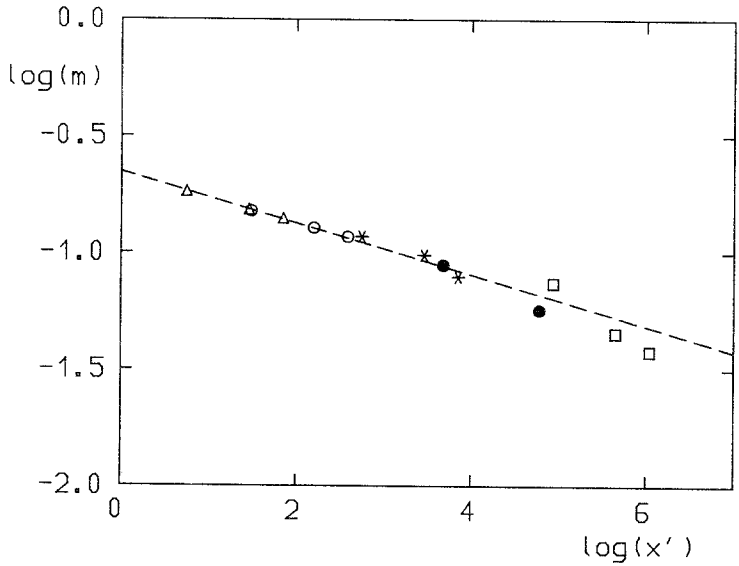

Fig. 11. Logarithmic representation of m_L versus $x' = \varepsilon' L^{1/\nu}$ above T_c^* to obtain β_s' and B_s' in Eq. (4.5). Same symbols as in Fig. 10.

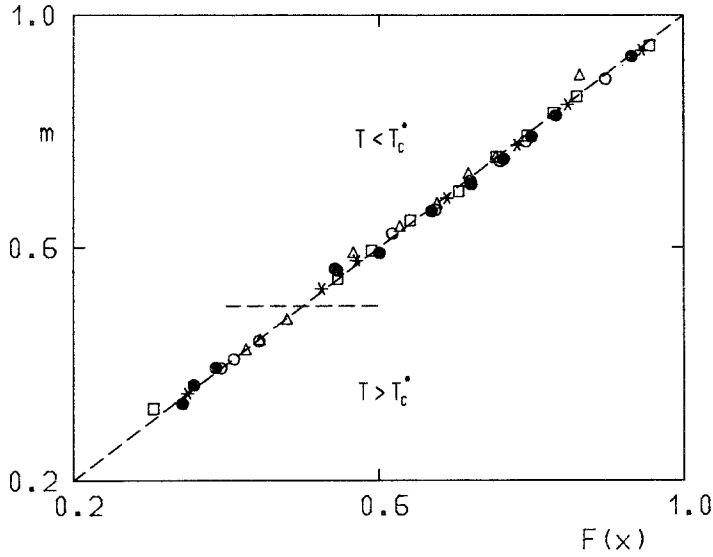

Fig. 12. The order parameter $m_L(T)$ against $F(x)$, defined as the rhs of Eqs. (4.4) and (4.5), using the parameters given in the text, to demonstrate the scaling behavior discussed in Section 4. Same symbols as in Fig. 10.

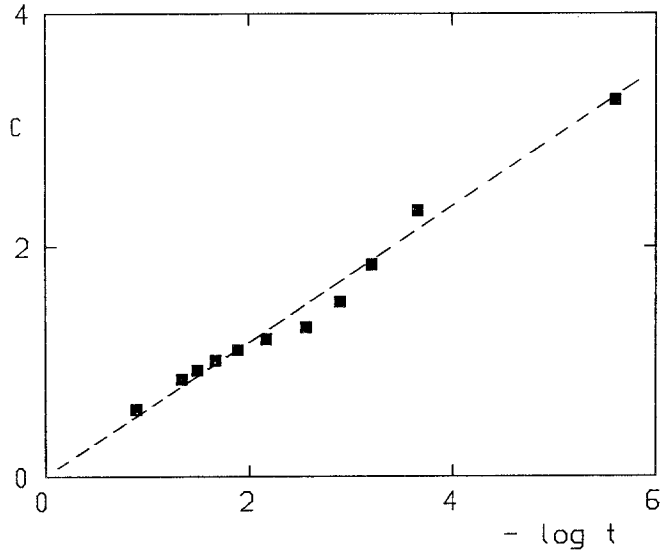

Fig. 13. Semilogarithmic plot of the specific heat for the infinite lattice (Fig. 7) versus $\ln \varepsilon$, showing the consistency of the data with a logarithmic divergence.

quantities (Section 3) is rather involved and the resulting indirect data are too noisy to allow a definite conclusion as for m_L. On the other hand, referring to the case of the specific heat, the data obtained in Section 3 as an extrapolation for the infinite lattice lack the necessary quality to allow the direct evaluation of the corresponding critical exponent α; this is also hampered by the fact that $\alpha = 0$ for both the equilibrium Onsager solution (logarithmic divergence) and the mean-field theory (discontinuity). It is true, however, that Fig. 7 suggests a strong singularity of the specific heat at T_c^* and, in particular, that the data are consistent with this being a logarithmic singularity, as shown by Fig. 13; in any case, it should be mentioned that the precision of the data does not allow us to discard some small value for α. The ordering susceptibility in Fig. 8b, on the other hand, allows no conclusion about γ.

5. CORRELATIONS

As discussed before, of particular interest in the present problem is the detailed study of correlation functions along the two principal directions of the lattice. Unfortunately, the MC method is not the most suitable for that purpose, e.g., finite-size effects below T_c^* may even influence the qualitative nature of the correlation functions, and the underlying theory is less developed than for the critical behavior of other quantities, etc.; in any case, their study provides some interesting qualitative and semiquantitative features of the model.

The relevant quantities are the longitudinal (along the field direction) and transverse (perpendicualr to it) pair correlation functions defined, respectively, as the ensemble average of

$$g_l(r) = N^{-1} \sum_{i,j}^{L} (2n_{ij} - 1)(2n_{i+r,j} - 1) - \eta^2 \tag{5.1a}$$

where $\eta = 2\rho - 1$ and i represents the index describing the $\hat{x}$ direction, and

$$g_t(r) = N^{-1} \sum_{i,j}^{L} (2n_{ij} - 1)(2n_{i,j+r} - 1) - \eta^2 \tag{5.1b}$$

with j describing the direction perpendicular to the field. The computations refer to the $L = 100$ lattice and $\eta = 0$.

Figure 14 collects some representative results, whose interpretation is rather simple. The longitudinal correlation decreases with r rather quickly from the value $g_l(0) = 1$ until a constant value, which decreases with

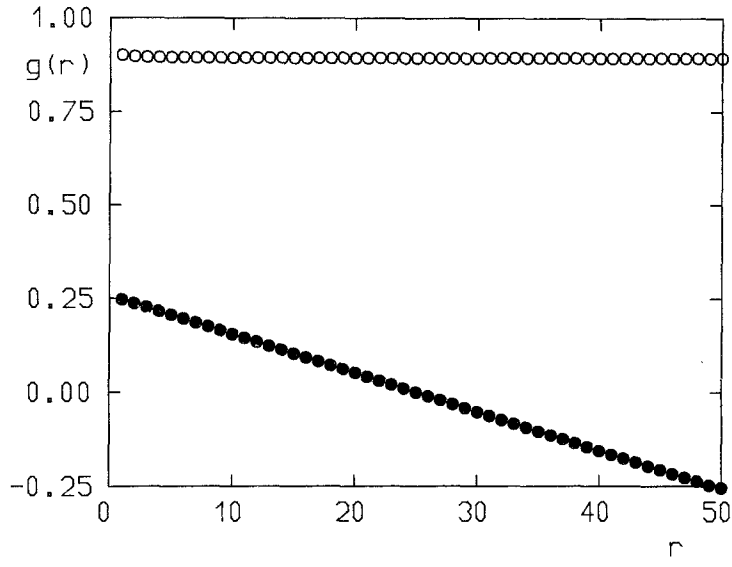

(a)

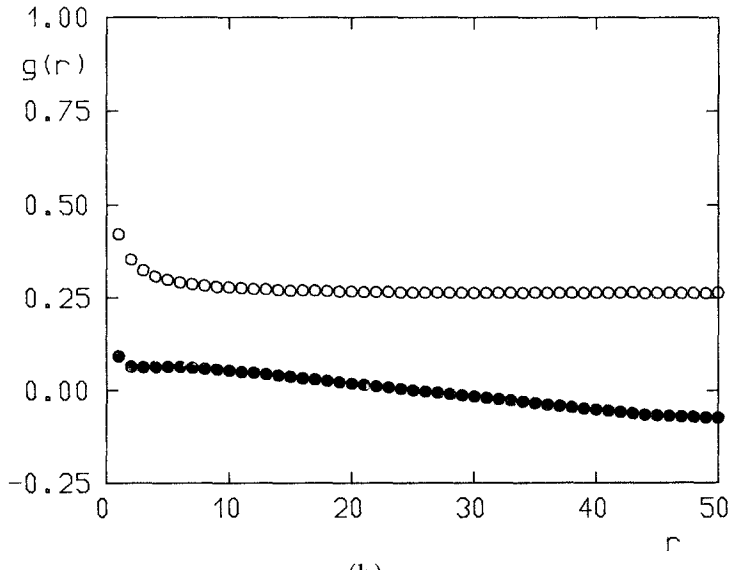

(b)

Fig. 14. (○) Longitudinal and (●) transverse correlation functions as defined by Eqs. (5.1): (a) during the stationary state at $T=0.8T_c \ll T_c^*$, (b) at $T=1.32T_c \lesssim T_c^*$, (c) at $T=1.45T_c > T_c^*$, and (d) in the case of intermediate states with several strips, as in Fig. 1e, at $T=1.1T_c$.

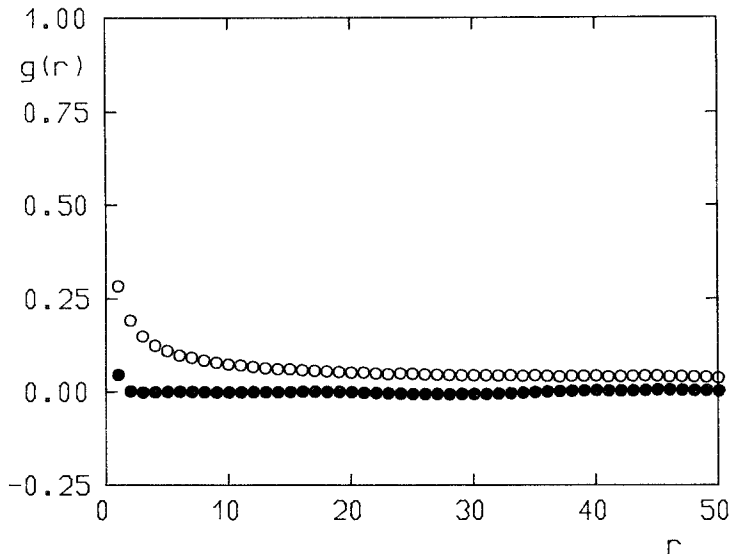

(c)

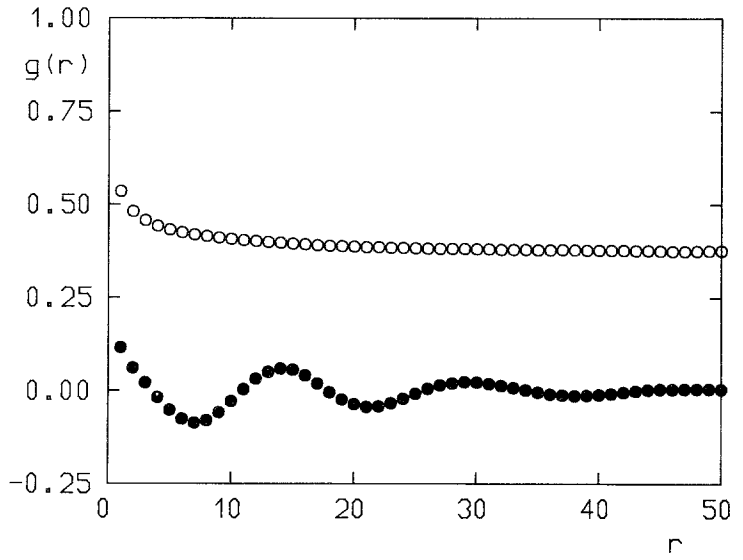

(d)

Fig. 14 (*continued*)

increasing temperature (Fig. 15), this also being the case for intermediate multistrip states. The transverse correlation, on the contrary, usually reflects a richer structure associated with the phase segregation in the system. The system in Fig. 14a presents a very well-defined strip of particles, and $g_t(r)$ decreases with r, reaching a zero at $L/4$ and the minimum value at $L/2$, the width of the strip; this behavior is less pronounced in Fig. 15b, where the strip is not so well defined, and $g_t(r)$ is practically negligible above T_c^* in Fig. 14c. Figure 14d corresponds to states such as the one represented in Fig. 1e with seven rather well-defined strips, and $g_t(r)$ clearly reveals that structure.

As expected, the correlation function is indeed highly anisotropic and, at a given temperature, the longitudinal correlation function is always higher than the transverse one; this effect is more pronounced as the temperature is lowered, but is also noticeable above T_c^*.

The latter fact deserves a closer inspection. Actually, Fig. 1d reveals the presence of a high degree of anisotropic order at $T = 1.45T_c$, above T_c^* $(= 1.355T_c)$. The effect is still very evident well above T_c^*, as in Fig. 16, showing the presence of clusters, which are predominantly oriented in the direction of the field at $T \geqslant 2T_c^*$. That is, it seems that the (infinite) field is enhancing the longitudinal correlations so much that it is capable of causing some important ordering at relatively high temperatures, even

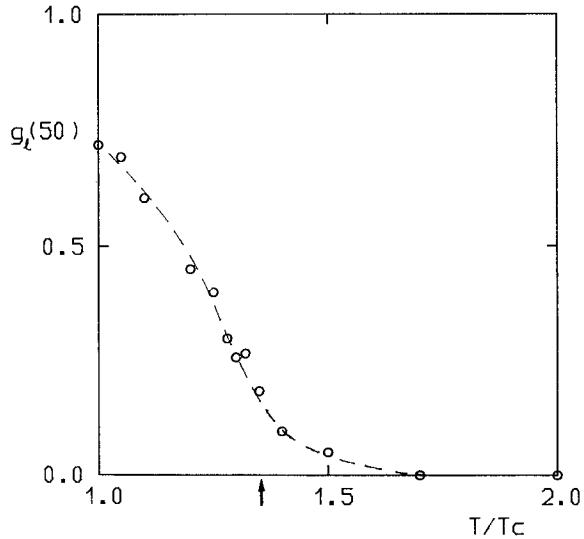

Fig. 15. Value of the longitudinal correlation function $g_t(r)$ for $r = L/2$ $(L = 100)$ as a function of temperature. These values are also given in Table I as a_3. The arrow locates T_c^*.

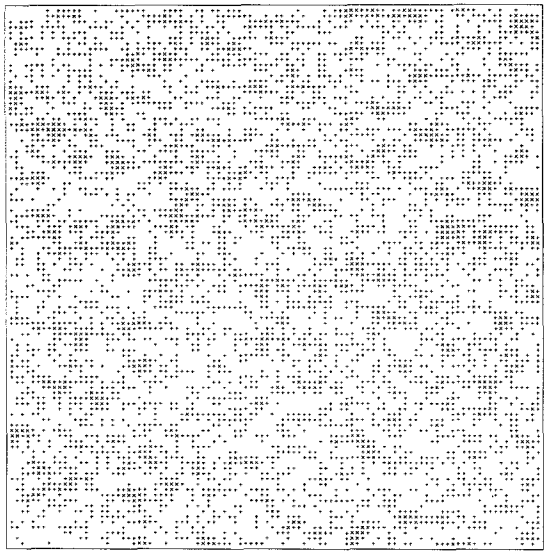

(a)

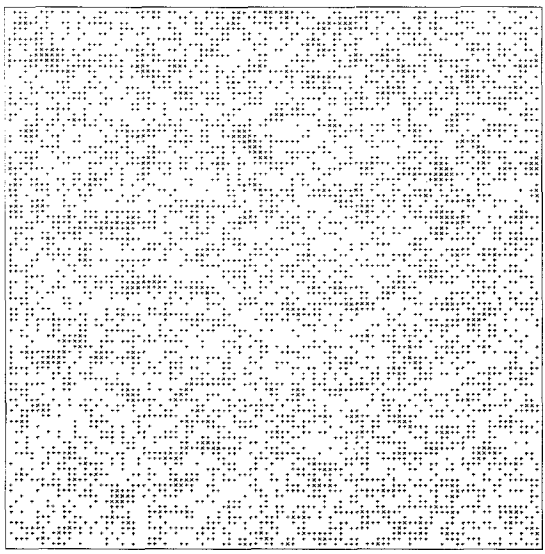

(b)

Fig. 16. A comparison of several typical configurations showing the presence of some anisotropic clustering well above T_c^* in the presence of the (infinite) field: (a) $T=2T_c$, $L=100$, (b) $T=3T_c$, $L=100$, (c) infinite temperature with no field, $L=120$. See also Fig. 1d.

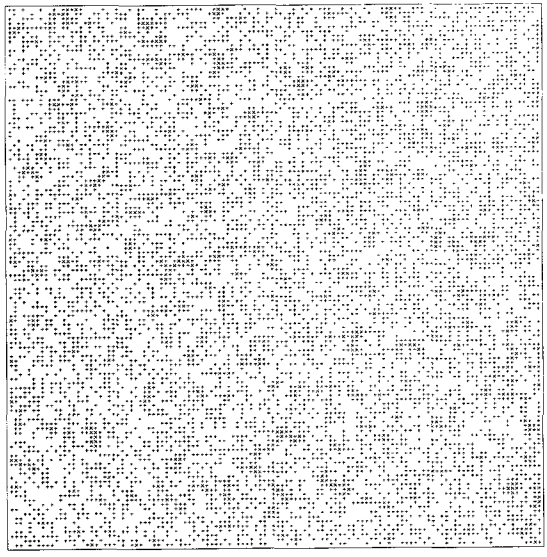

(c)

Fig. 16 (*continued*)

much higher than the temperature for the onset of well-segregated strip states, where the equilibrium ($E=0$) configurations would be practically indistinguishable from the infinite-temperature ones; cf. Figs. 16 and 1d.

In order to look more closely at this effect, and try to confirm our previous statements about the correlation length critical exponent, we have analyzed numerically the directional kcorrelation lengths above T_c^*, where finite-size effects are negligible in practice. Some of the corresponding data for the longitudinal and transverse cases are collected in Figs. 17 and 18 and in Table I.

The initial (small-r) strong decay shown vy the transverse correltion function (Fig. 17a) can be fitted by using an exponential,

$$g_t(r) \approx e^{-r/\xi}, \qquad \text{small } r, \quad T > T_c^* \tag{5.2}$$

with $\xi = \xi(T)$ decreasing monotonically with increasing T (Table I). The longitudinal correlations, on the other hand, decay much more slowly, as shown by Fig. 17b. Motivated by the equilibrium theory, we tried several expressions to describe the data in Fig. 17b. We only mention the fit $g_l(r) \approx A \exp(-r/\xi) e^{-b}$; this is rather poor, but it produces the interesting result b ($\equiv d-2+\eta$) $=0.11$, independent of temperature, which is intermediate between the Onsager ($\eta = 1/4$) and classical ($\eta = 0$) results, as occurs with other critical exponents reported in this paper.

Table I. Values of the Parameters for Eqs. (5.2) and (5.3)

T/T_c	1.0	1.05	1.1	1.2	1.25	1.28	1.3	1.32	1.35	1.4	1.5	1.7	1.8	1.9	2.0	2.2	2.5	3.0	4.0
ξ	—	—	—	—	—	—	—	—	—	0.36	0.33	0.28	0.27	0.26	0.25	0.25	0.24	0.22	0.21
l	0.37	0.39	0.42	0.40	0.42	0.46	0.44	0.43	0.47	0.45	0.46	0.44	0.42	0.40	0.37	0.35	0.31	0.28	0.24
λ	3.6	4.7	4.4	3.1	3.3	4.4	4.2	3.7	4.6	4.5	4.7	3.8	3.3	2.9	2.6	2.3	2.0	1.5	1.2
a_1	0.26	0.29	0.36	0.47	0.52	0.61	0.63	0.63	0.70	0.76	0.80	0.86	0.86	0.86	0.86	0.86	0.86	0.86	0.86
a_3	0.72	0.69	0.60	0.45	0.40	0.30	0.26	0.27	0.18	0.10	0.05	0	0	0	0	0	0	0	0

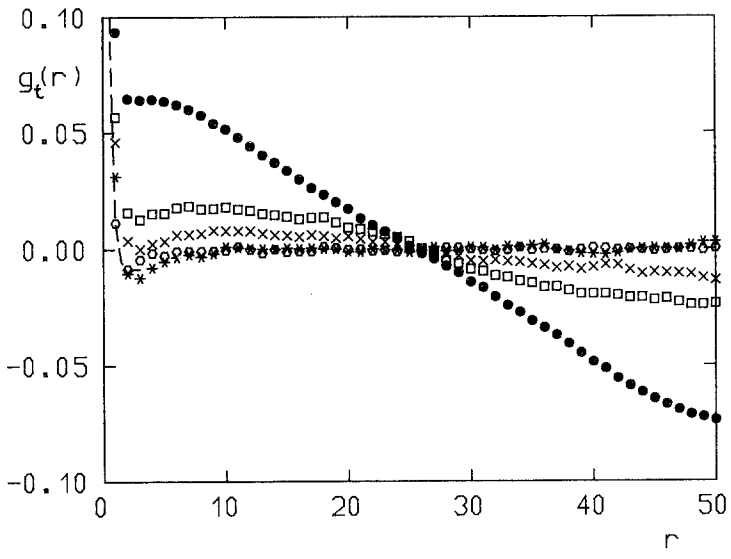

(a)

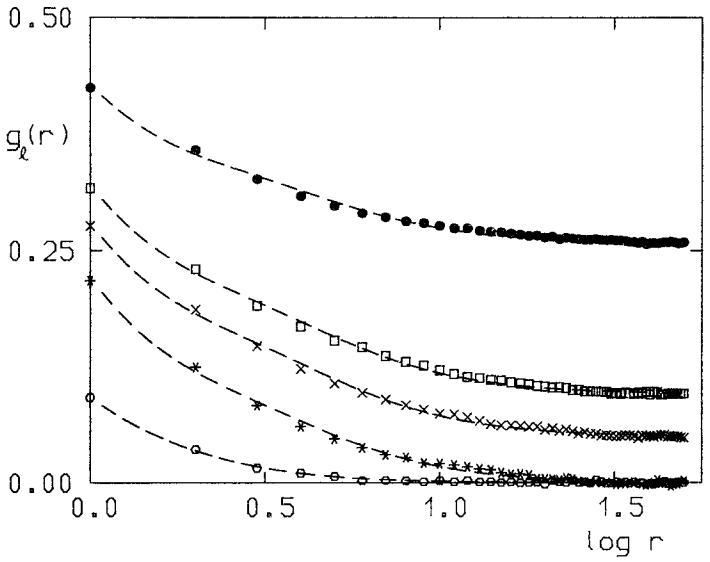

(b)

Fig. 17. Correlation functions for $T \gtrsim T_c^*$. Here $T = (\bullet)\, 1.3T_c$, $(\square)\, 1.4T_c$, $(\times)\, 1.5T_c$, $(*)\, 1.7T_c$, and $(\circ)\, 4T_c$. (a) Transverse case as a function of r; the dashed line represents an exponential fit as in Eq. (5.2). (b) Longitudinal case as a function of $\log_{10} r$; the dashed lines correspond to the behavior (5.3).

Assuming that the data in Fig. 17b cannot be described by a single simple behavior, it seems interesting to mention the phenomenological fit

$$g_l(r) = a_1 e^{-r/l} + a_2[1 + (r/\lambda)^2]^{-1} + a_3 \tag{5.3}$$

where a_i are temperature-dependent parameters satisfying the normalization condition $a_1(T) + a_2(T) + a_3(T) = 1$. This, implying a change over of $g_l(r)$ with r, adjusts the data for $T > T_c^*$ very well when on sets $a_3 = g_l(r = L/2)$ and uses l, λ, and a_1 as adjustable parameters (Fig. 17b); it is interesting that Eq. (5.3) also describes very well the data below T_c^*. Table I lists the values for the parameters in Eq. (5.3). On the other hand, Table I reveals that $\xi \approx l$ for $T > T_c^*$, so that one also has

$$g_l(r) - g_t(r) = A[1 + (r/\lambda)^2]^{-1}, \qquad r > l \tag{5.4}$$

which is indeed confirmed independently by the data for $T > T_c^*$. These facts seem to be consistent with our assumption about a single correlation length in the system.

As shown by Figs. 17b and 15, and by the values for $a_3 \equiv g_l(r = L/2)$ in Table I, $g_l(r)$ has a nonzero value at large r even for some temperatures above T_c^* (e.g., at $T > 1.5T_c$), revealing the existence of some long-range order, probably due to some finite-size effect. This is consistent with the existence of anisotropic clustering, i.e., clusters of ions having a longitudinal size larger than the transverse one, which can be observed very

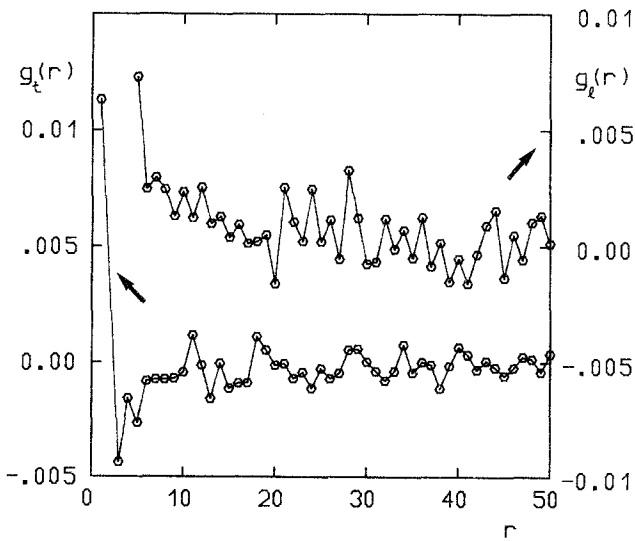

Fig. 18. Detail of the tails of the directional correlation functions in the case $T = 4T_c$.

clearly at $2T_c$ and even at highr temperature; cf. Figs. 1d, 16a, and 16b. This is also revealed by Fig. 18, representing the tail of $g(r)$ with great detail at $T=4T_c$: $g_l(r)$ and $g_t(r)$ show indeed a different behavior at such high temperatures.

6. CONCLUSION

The model considered in this paper allows the study of nonequilibrium second-order phase transitions and stationary states. Concerning the latter, the apparent breakdown of dissipation-fluctuation theorems is revealed. Concerning the former, we have performed a detailed finite-size scaling analysis, which confirms our previous[6] arguments favoring a novel critical behavior for the infinite system, which differs from both the equilibrium and the classical ones, in the case of two dimensions. The scaling behavior found also has an intrinsic interest: it essentially deviates from the one for the equilibrium Ising model (no electric field) with periodic boundary conditions, the kind of boundary conditions considered for the model here, when one makes the assumption that, in spite of the great anisotropy of our model, there is only a *relevant* correlation length in the problem. This is motivated and it also seems confirmed by an independent study of correlation functions. It should bementioned that our observation of an *effective* correlation length may perhaps raise some doubts about (though it does not necessarily exclude) the recent assumption[11–13] of well-defined longitudinal and transverse correlation lengths which behave differently as one approaches the critical temperature. The computer simulations and, in particular, our study of correlation functions indicate as well the presence of some order (anisotropic clustering) above the nonequilibrium critical temperature, a fact that deserves more thought. Actually, the most general conclusion concerning correlations in the present model is that there remain a number of questions to be answered; much more work will be needed for that purpose; e.g., it turns out that it may be useful to perform further computations referring to square, rectangular, and three-dimensional lattices. We are carrying out a finite-size scaling analysis of the three-dimensional versions of the model.

The critical behavior of the present model seems to deviate from that in related models[2,3,8–13]; this is a manifestation of the fact that the nonequilibrium critical behavior is much more complex and varied than the equilibrium counterpart. While this should be expected given the singular simplicity of the equilibrium state, it might be considered a surprise at a time when the Landau theory is recognized as bearing great relevance in the description of nonequilibrium phase transitions. This "surprise" should motivate related experimental work.

ACKNOWLEDGMENTS

This work was partially supported by the U.S.–Spanish Cooperative Research Program under grant CCB-8402025 and by the CAICYT under Project PB85-0062, Spain.

NOTE ADDED IN PROOF

Due to an inadvertent error, the values of the transversal correlations in Figs. 14, 17a, and 18 need to be multiplied by a factor of 25/7, and the values of ξ in Table I need to be modified accordingly.

REFERENCES

1. J. Marro and J. L. Vallés, *J. Stat. Phys.*, this issue, next paper.
2. H. van Beijeren and L. S. Schulman, *Phys. Rev. Lett.* **53**:806 (1984).
3. J. Krug, J. L. Lebowitz, H. Spohn, and M. Q. Zhang, *J. Stat. Phys.* **44**:535 (196).
4. S. Katz, J. L. Lebowitz, and H. Spohn, *Phys. Rev. B* **28**:1655 (1983); *J. Stat. Phys.* **34**:497 (1984).
5. J. Marro, J. L. Lebowitz, H. Spohn, and M. H. Kalos, *J. Stat. Phys.* **38**:725 (1985).
6. J. L. Vallés and J. Marro, *J. Stat. Phys.* **43**:441 (1986).
7. J. Marro *et al.*, unpublished.
8. A. Onuki and K. Kawasaki, *Ann. Phys. (N.Y.)* **131**:217 (1981), and references therein.
9. A. de Masi, P. A. Ferrari, and J. L. Lebowitz, *Phys. Rev. Lett.* **55**:1947 (1985); *J. Stat. Phys.* **44**:589 (1986).
10. J. Marro, J. L. Vallés, and J. M. González-Miranda, *Phys. Rev. B* **35**:000 (1987).
11. K. Gawedzki and A. Kupiainen, preprint (1986).
12. K. Leung and J. L. Cardy, *J. Stat. Phys.* **44**:567 (1986).
13. H. K. Janssen and B. Schmittmann, preprint (1986).
14. M. E. Fisher, in *Critical Phenomena*, M. S. Green, ed. (Academic Press, New York, 1971); K. Binder and P. C. Hohenberg, *Phys. Rev. B* **6**:3461 (1972); D. P. Landau, *Phys. Rev. B* **13**:2997 (1976); T. Graim and D. P. Landau, *Phys. Rev. B* **24**:5156 (1981).
15. S. R. de Groot and P. Mazur, *Nonequilibrium Thermodynamics* (Dover, New York, 1984).
16. S. Katz, private communication.
17. A. E. Ferdinand and M. E. Fisher, *Phys. Rev.* **185**:832 (1969); see also M. N. Berber, in *Phase Transformations and Critical Phenomena*, Vol. 8, C. Domb and J. L. Lebowitz, eds. (Academic Press, New York, 1983).